Journal of Histochemistry & Cytochemistry 60(1) 22–30

DOI: 10.1369/0022155411425389
http://jhc.sagepub.com
SAGE

Immunolocalization of Myostatin (GDF-8) Following Musculoskeletal Injury and the Effects of Exogenous Myostatin on Muscle and Bone Healing

Moataz Elkasrawy, David Immel, Xuejun Wen, Xiaoyan Liu, Li-Fang Liang, and Mark W. Hamrick

School of Dental Medicine, University of Colorado Denver, Denver, Colorado (ME); Savannah River National Laboratory, Aiken, South Carolina (DI); Clemson University and Medical University of South Carolina Bioengineering Program, Charleston, South Carolina (XW, XL); MetaMorphix, Inc, Calverton, Maryland (L-FL); and Georgia Health Sciences University, Augusta, Georgia (ME, MWH)

Summary

The time course and cellular localization of myostatin expression following musculoskeletal injury are not well understood; therefore, the authors evaluated the temporal and spatial localization of myostatin during muscle and bone repair following deep penetrant injury in a mouse model. They then used hydrogel delivery of exogenous myostatin in the same injury model to determine the effects of myostatin exposure on muscle and bone healing. Results showed that a "pool" of intense myostatin staining was observed among injured skeletal muscle fibers 12–24 hr postsurgery and that myostatin was also expressed in the soft callus chondrocytes 4 days following osteotomy. Hydrogel delivery of 10 or 100 µg/ml recombinant myostatin decreased fracture callus cartilage area relative to total callus area in a dose-dependent manner by 41% and 80% ($p<0.05$), respectively, compared to vehicle treatment. Myostatin treatment also decreased fracture callus total bone volume by 30.6% and 38.8% ($p<0.05$), with the higher dose of recombinant myostatin yielding the greatest decrease in callus bone volume. Finally, exogenous myostatin treatment caused a significant dose-dependent increase in fibrous tissue formation in skeletal muscle. Together, these findings suggest that early pharmacological inhibition of myostatin is likely to improve the regenerative potential of both muscle and bone following deep penetrant musculoskeletal injury. (J Histochem Cytochem 60:22–30, 2012)

Keywords

muscle regeneration, endochondral ossification, fracture healing, fibrosis

Myostatin (GDF-8) is most well recognized as a factor that has potent catabolic and anti-anabolic effects on skeletal muscle (Lee 2004). Myostatin levels are elevated in conditions associated with muscle atrophy, such as cancer cachexia (Zimmers et al. 2002; Reisz-Porszasz et al. 2003) and unloading (Wehling et al. 2000; Allen et al. 2009), and blocking myostatin function can increase muscle mass and improve muscle regeneration (McPherron et al. 1997; Whittemore et al. 2003; Wagner, 2005). Skeletal muscle is known to have important effects on bone healing (Stein et al. 2002; Hamrick, McNeil, et al. 2010; Hamrick, 2011). For example, muscle flaps are often used to promote and accelerate fracture repair (Gopal et al. 2000), and significant damage to muscle tissue following traumatic orthopaedic injury is believed to delay and retard the normal fracture healing process (Utvag et al. 2002). Thus, while muscle is known to play a key role in fracture healing and myostatin plays an important role in muscle regeneration, the role of myostatin in regulating musculoskeletal injury repair remains poorly understood.

Myostatin was previously found to be highly expressed during the early stages of fracture healing (Cho et al. 2002),

Received for publication June 1, 2011; accepted September 8, 2011.

Corresponding Author:
Mark W. Hamrick, PhD, Department of Cellular Biology and Anatomy, Georgia Health Sciences University, Cb1116 Laney Walker Blvd, Augusta, GA 30912
E-mail: mhamrick@georgiahealth.edu

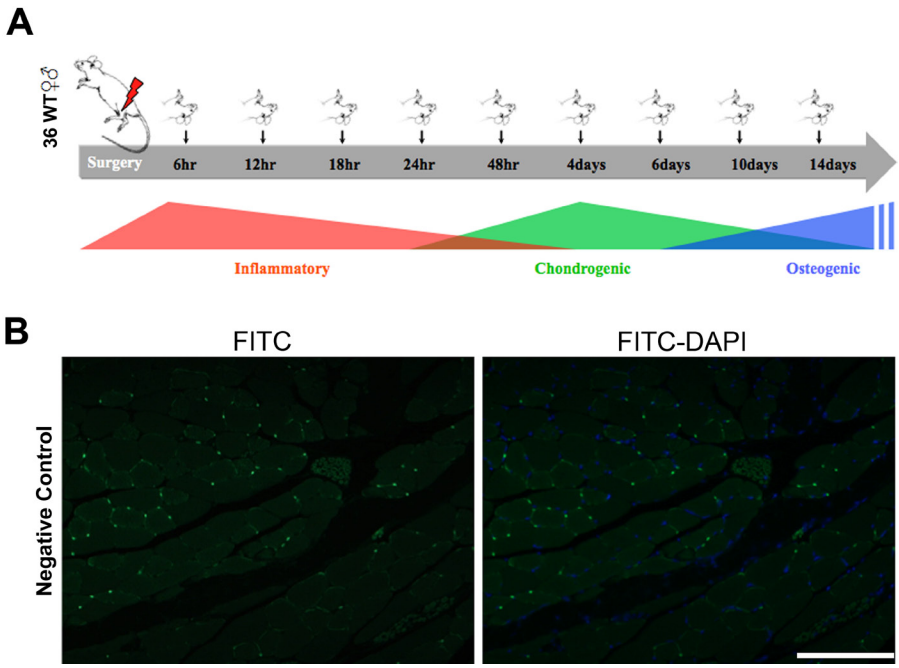

Figure 1. (A) General phases of fracture healing and time points examined for immunohistochemical staining of myostatin. (B) Negative control sections of skeletal muscle stained with FITC-conjugated secondary antibody but not primary antibody. Scale bar = 100 µm.

and fracture callus size was observed to be significantly greater in myostatin-deficient mice compared to wild-type controls (Kellum et al. 2009). Moreover, blocking myostatin signaling using a recombinant myostatin propeptide appears to enhance muscle and bone healing following fibula osteotomy and muscle injury in mice (Hamrick, Arounleut, et al. 2010). These findings all point to an important role for myostatin in muscle and bone regeneration, but several outstanding questions remain. First, it is well established that the receptor for myostatin, the type IIB activin receptor (ActRIIB, or Acvr2b), is expressed in bone marrow–derived stromal cells (Hamrick et al. 2007), osteoblasts (Shuto et al. 1997), myoblasts (Ostebye et al. 2007), fibroblasts (Li et al. 2008; Mendias et al., 2008; Fulzele et al., 2010), and chondrocytes (Nagamine et al. 1998), but what is the source of myostatin? In other words, is myostatin expressed in an autocrine fashion by marrow stromal cells and chondrocytes, or is myostatin secreted primarily by muscle cells, which affect chondro- and osteoprogenitors in a paracrine fashion? Second, what is the time course of myostatin expression following musculoskeletal injury? This question is particularly relevant because if myostatin inhibitors are to be delivered as potential therapeutics, then their efficacy may be highly dependent upon the time at which they are administered. Finally, what are the effects of exogenous myostatin on muscle and bone healing? If blocking myostatin is thought to enhance tissue repair and regeneration, then the converse is also expected to be true. That is, exposure to recombinant myostatin would be expected to suppress or impair normal healing.

We addressed these outstanding questions using the following approaches. First, we used a time course immunohistochemical study in normal wild-type mice to localize those cells expressing myostatin in situ following musculoskeletal injury. We then used an experimental approach to deliver exogenous myostatin directly to the injury site following surgery. These studies shed new light on the role of myostatin in musculoskeletal tissue repair.

Materials And Methods

Animals

Thirty-six wild-type (CD-1) mice 3–4 months of age were used to analyze the temporal and spatial expression of myostatin during fracture healing using immunohistochemistry. Mice were randomly divided into nine groups, each undergoing fibular osteotomy on one leg with transection of the surrounding lateral compartment muscles. Mice were then euthanized at different time points spanning the inflammatory, chondrogenic, and early osteogenic phases of fracture healing: 6, 12, 18, 24, 48 hr and 4, 6, 10, 14 days after fracture (Fig. 1A). Thirty-three adult wild-type (CD-1) mice 3–4 months of age were used for experiments where myostatin was injected directly into the injury site following osteotomy and muscle transection. For these experiments, mice were randomly

divided into three groups, each group receiving an increasing dose (0, 10, 100 μg/ml) of recombinant myostatin (cat. No. AF788; R&D Systems) loaded in a biodegradable hydrogel injection at the fracture site. Details of the hydrogel formulation are provided below. Mice were euthanized 15 days after surgery using CO_2 overdose followed by thoracotomy. Body weights were measured before surgery and following sacrifice. Mice were purchased from Charles River Laboratories and were housed in the same room and given food and water ad libitum. All procedures were performed with Institutional Animal Care and Use Committee approval.

Fibular Osteotomy and Tissue Preparation

The fibula osteotomy procedure with injury to surrounding lateral compartment muscles follows the general procedure that we have described elsewhere (Hamrick, Arounleut, et al. 2010b). Briefly, mice were anesthetized using isoflurane, and the lateral side of the hind leg was shaved with a hair clipper and disinfected with Betadine, followed by 70% ethyl alcohol. A longitudinal 5-mm skin incision was made along the lateral side of the right leg approximately 10–12 mm proximal to the calcaneal tuberosity, and the fibularis longus and brevis were cut transversely to expose the fibula. A transverse fracture was made at the middle of the fibula using microtenotomy scissors, and the surgical wound was closed using skin glue (3M Vetbond). Twenty mg/kg of anti-inflammatory Ketorolac was administered intraperitoneally immediately and 24 hr after surgery (for groups 48 hr postfracture and later). Mice were euthanized using CO_2 overdose, followed by thoracotomy; legs were disarticulated at the knee and ankle joints; and skin was removed gently to avoid disrupting the callus. Specimens were then fixed in 4% paraformaldehyde at 4C. After 24 hr, the specimens were washed in 1× PBS and preserved in 70% ethyl alcohol at 4C. Following microcomputed tomography (microCT), the specimens were then decalcified by immersing in 0.1M EDTA at pH 7.4 for 5 weeks at 4C. Tissues were dehydrated in graded ethyl alcohol, embedded in paraffin, sectioned transversely at the center of fracture at 7-μm thickness, and mounted on Frost Plus glass slides (Fisher).

Immunohistochemistry

Paraffin sections were deparaffinized, hydrated, permeabilized in 0.2% Triton ×100 in a 1× PBS solution for 10 min, and heated for epitope retrieval in citrate buffer solution pH 6.0 (Invitrogen) on a hot plate (95C) for 15 min. Nonspecific binding was blocked with 10% normal goat serum (Vector Laboratories) in 0.1% Triton ×100 in a 1× PBS solution for 1 hr at room temperature in a humidifying chamber. Serial sections were incubated with primary polyclonal antibodies against myostatin (rabbit anti-myostatin; AB3239, Millipore) at 1:50 dilution in 0.1% Triton ×100 in a 1× PBS solution overnight at 4C in the humidifying chamber. Before undertaking this study, we compared four myostatin antibodies from three manufacturers: Santa-Cruz, Millipore, and R&D Systems. We selected the Millipore antibody for two reasons. First, this antibody is immunoaffinity purified; second, it is well documented (e.g., Gonzalez-Cadavid et al. 1998; Hittel et al. 2010) to recognize the mature form of myostatin. After being washed with 1× PBS three times for 3 min, sections were incubated with secondary antibody (goat anti-rabbit; AlexaFluor-488, Invitrogen) for 1 hr at room temperature in the humidifying chamber. Finally, the sections were stained with 4′,6-diamidino-2-phenylindole (Vector Laboratories) nuclear stain and coverslipped with Vectashield mounting medium (Vector Laboratories). Primary antibody was omitted for sections used as negative controls (Fig 1B). Serial sections were stained with hematoxylin and eosin. Images were captured on a Carl Zeiss fluorescence microscope using AxioVision Image Analysis software, version 08.2008.

Hydrogel Delivery of Exogenous Myostatin to the Fibula Osteotomy Site In Vivo

The fibular osteotomy procedure was performed as described above, and a gastight glass syringe (Luer tip; 1700 Series, Hamilton Syringes) was used to inject 30 μl of hydrogel loaded with 0 (1× PBS), 10, or 100 μg/ml recombinant myostatin at the fracture site immediately following osteotomy. The hydrogel consisted of a proprietary formulation of thiolated hyalyronan, thiolated gelatin, thiolated chitosan, and poly (ethylene glycol) tetraacrylate. The gelation was triggered by adding the crosslinker [poly (ethylene glycol) tetraacrylate] to the mixture of thiolated hyalyronan, thiolated gelatin, and thiolated chitosan. A protease inhibitor cocktail was added to prevent degradation of the recombinant myostatin. The 1× protease inhibitor cocktail consists of PIC1 and PIC2 (1000×; PIC1: 1 mg/ml of leupeptin, 2 mg/ml of antipain, and 10 mg/ml of benzamidine dissolved in 10,000 U/ml of aprotinin; PIC2: 1 mg/ml of chymostatin and 1 mg/ml of pepstatin dissolved in dimethyl sulfoxide). Before the addition of the crosslinker, recombinant myostatin was added to the mixture at myostatin concentrations of 0 (1× PBS), 10, or 100 μg/ml. After 15 days, mice were euthanized with Institutional Animal Care and Use Committee protocol approval, using CO_2 overdose followed by thoracotomy. Legs were fixed and processed for microCT imaging and histology as described above.

MicroCT Analysis of Fracture Healing

MicroCT imaging was performed at the Savannah River Site National Laboratory (Aiken, South Carolina) using a 160-kV microfocus X-ray machine (Model 16010, Kevex Inc), a four-axis positioning system (Series 300, New

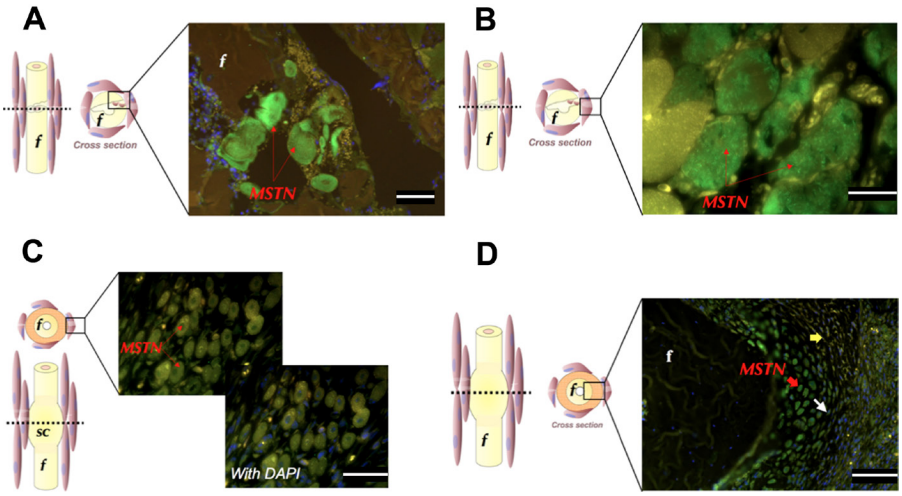

Figure 2. Immunohistochemistry staining (green fluorescence) of myostatin in transverse section of fracture site. Left-panel figures indicate plane of section and area of interest shown in micrograph. Injured skeletal muscle fibers highly express myostatin at 12 hr (A; scale bar = 25 µm) and 24 hr (B; scale bar = 10 µm) following surgery. Six days postfracture, high myostatin expression (arrow) is restricted to the nuclei of regenerating myotubes (C; scale bar = 25 µm). Four days postfracture, round, mature soft callus chondrocytes (red arrow) and flat proliferating chondrocytes (white arrow) express myostatin (D; scale bar = 50 µm). Sections are counterstained with DAPI, and blue DAPI staining is abundant in the bottom right quadrant of the image (D). f, fibula; MSTN, myostatin; sc, soft callus. Yellow arrows indicate chondroprogenitor cells. Yellow staining represents autofluorescence.

England Affiliated Technologies), and an amorphous silicon imager (Paxscan 4030; Varian Inc) at 12-µm resolution as described previously (Kellum et al. 2009; Hamrick, Arounleut, et al. 2010). Measurements of total callus volume and callus bone mineral density were calculated 0.5 mm on either side of the callus center.

Histology and Histomorphometric Analysis of Fracture Healing

Specimens were decalcified using 0.1M EDTA, embedded in paraffin, and sectioned at 7 µm. To quantify the area of endochondral bone formation, paraffin sections were stained with safranin O and fast green, which stains the proteoglycan of cartilage an orange red and the background green. To quantify the degree of muscle regeneration, serial sections were stained using Masson's trichrome, which stains fibrous collagen-rich tissue blue and skeletal muscle red. A 0.8-mm^2 region of interest was examined lateral to the fibula fracture callus (Hamrick, Arounleut, et al. 2010), and the relative fraction of blue to red pixels in each image was quantified using NIH ImageJ 1.43r software. A higher-intensity value for the blue channel indicates that the image as a whole approximates pure blue; thus, the blue channel value represents an average of all pixels in that image rather than a total pixel number. We have estimated the percentage of fibrotic tissue to muscle as a ratio of the average "blueness" of the area of interest versus the average "redness." The images were captured using a QImaging digital camera at 40× and 100× for the Safranin O and Masson's trichrome staining, respectively.

Statistical Analysis

Results were plotted as mean ± SE. All statistical analysis was performed using Prism, version 5.0a. Multiple group comparisons were performed using one-way ANOVA. Post hoc analysis was performed using Newman-Keuls multiple comparison test. In all cases, statistical comparisons were considered significant at $p<0.05$.

Results

Myostatin staining is abundant among injured skeletal muscle fibers during the first 48 hr following surgery and in chondrocytes of the soft fracture callus 4 days following surgery. Myostatin expression was particularly noticeable among injured muscle fibers, both adjacent and away from the fracture site, 12 hr (Fig. 2A) and 24 hr (Fig. 2B) following surgery. A secreted "pool" of myostatin was most evident 12 hr following surgery close to injured muscle fibers around the osteotomy site (Fig. 2A). Muscle fibers that showed signs of degeneration, such as fragmentation, pyknotic nuclei, and disrupted plasma membranes, also showed marked expression of myostatin 6 days following injury (Fig. 2C). Occasional staining could be detected in the connective tissue around the fracture site up to 48 hr following fracture. Very weak signals were sporadically observed in

some periosteal and endosteal cells. On days 4, 6, and 10, the soft callus chondrocytes underwent several morphological and functional changes over the course of their life cycle during endochondral bone formation. By day 4, fibroblast-like spindle chondroprogenitor cells could be noticed toward the periphery of the cartilage island (Fig. 2D). Underneath the chondroprogenitor cell layer, flat proliferating and round mature chondrocytes, which are responsible for laying down cartilage matrix, could be identified. Myostatin was highly expressed in the round mature layer of chondrocytes and, to a lesser extent, in the flat proliferating chondrocytes (Fig. 2D). On days 6 and 10 following fracture, mature chondrocytes continued to stain strongly for myostatin.

Exogenous myostatin reduces chondrogenesis and fracture callus bone volume and impairs muscle regeneration in vivo. Hydrogel delivery of recombinant myostatin caused no significant decrease in mouse total body mass. The fracture callus showed a significant dose-dependent decrease in cartilage area and staining intensity with myostatin treatment (Fig. 3A). Cartilage area relative to total callus area decreased by 41% and 80% with 10 and 100 μg/ml of recombinant myostatin, respectively (Fig. 3B). MicroCT data showed a significant dose-dependent decrease in the bone volume in the fibula fracture callus with myostatin treatment of 38.8% and 30.6%, with the higher dose of recombinant myostatin yielding the greatest decrease in callus bone volume (Fig. 4A). Fracture callus total volume also decreased by 30% and 47% with 10 and 100 μg/ml of recombinant myostatin treatments, respectively (Fig. 4B). Histological sections of the fracture callus and surrounding muscle tissue stained with Masson's trichrome displayed signs of impairment in muscle regeneration, indicated by the significant increase in the degree of fibrous tissue formation (Fig. 5A). Myostatin treatment significantly decreased the fraction of fibrous tissue relative to muscle tissue by 16.2% and 10% with the high and low doses, respectively (Fig. 5B).

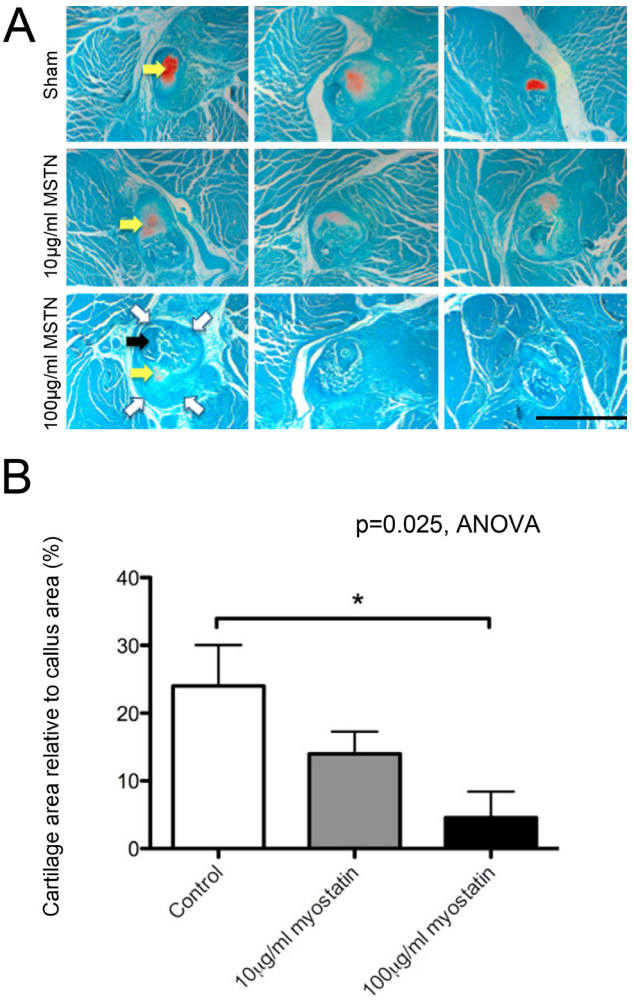

Figure 3. Endochondral ossification (orange stain, yellow arrows) is apparent at 15 days after fracture and is decreased by local treatment with recombinant myostatin. Light microscopic images of transverse sections in the center of 15-day-old fracture callus of myostatin-treated mice, stained with Safranin O and fast green. Fracture callus outline is indicated by open white arrows and cortical bone of the fractured fibula by the solid black arrow (A; scale bar = 500 μm). Cartilage area relative to total callus area decreased in a dose-dependent manner with myostatin treatment (B; n=5–7 per group). MSTN, myostatin.

Discussion

Myostatin is widely recognized as a potent suppressor of muscle growth, development, and regeneration. Recent studies have also noted a link between myostatin and bone formation. For example, mice lacking myostatin show an increase in bone density and strength (Elkasrawy and Hamrick 2010); blocking myostatin using systemic injections of a myostatin inhibitor causes enhanced bone regeneration (Hamrick, Arounleut, et al. 2010b); and fracture callus volume is increased in myostatin-deficient mice (Kellum et al. 2009). However, our knowledge of the mechanism by which myostatin regulates bone formation is lacking. A major question that remains unanswered is whether such effects on bone formation are indirect manifestations of increased muscle mass or are direct effects of myostatin on bone tissue. The data presented here point to both autocrine and paracrine effects of myostatin during fracture healing. Specifically, the early and consistent expression of myostatin in the injured muscles immediately adjacent to the fractured bone suggests that myostatin is made available in the milieu of the fracture site by injured muscle fibers and regenerating myotubes. This finding is consistent with results showing that extensive muscle tissue defects have a negative impact on early bone healing (Utvag et al. 2002) and with previous data demonstrating that peak levels of myostatin expression

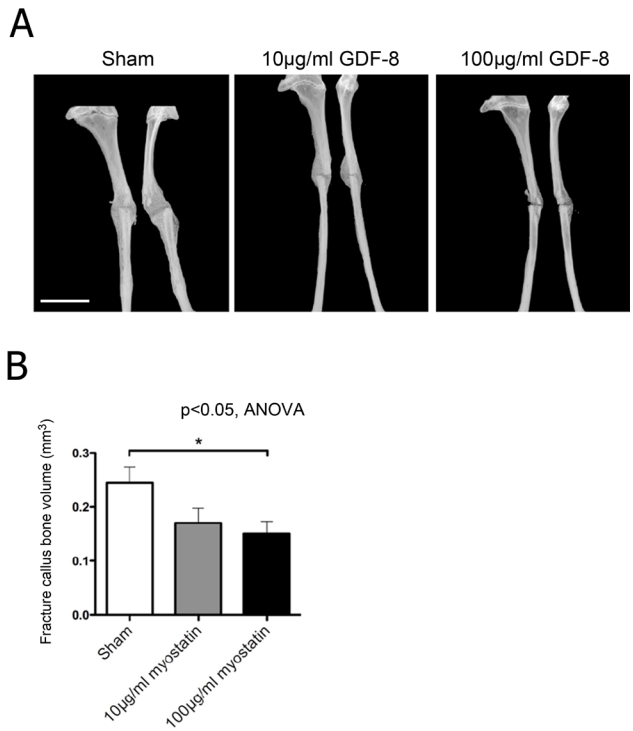

Figure 4. Fracture callus bony union (non-lamellar) is formed at 15 days after fracture and is decreased by local treatment with recombinant myostatin. Microcomputed tomography images of the fracture callus in the mouse fibula, treated with increasing doses of myostatin. Mediolateral (left) and anteroposterior (right) views (A; scale bar = 2 mm). Fracture callus bone volume decreased with myostatin treatment (B; *n*=9–11 per group). GDF-8, myostatin.

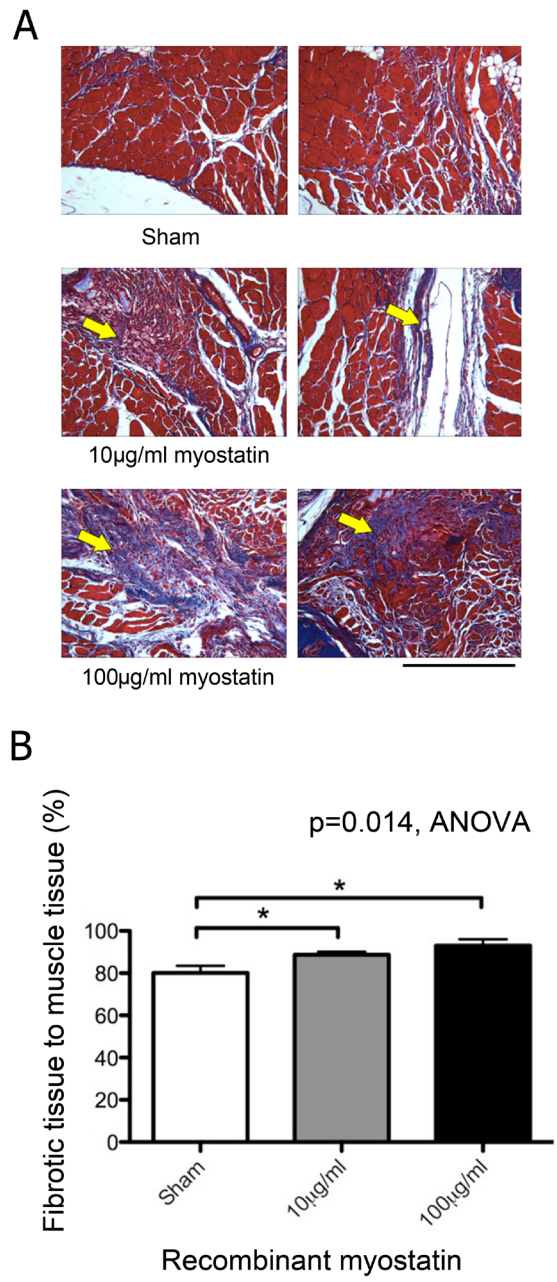

Figure 5. Fibrous tissue formation in local myostatin-treated mice. Histological sections stained with Masson's trichrome showing a dose-dependent increase in fibrous tissue formation (blue stain, arrow) during muscle repair with myostatin treatment (A; scale bar = 500 µm). Myostatin treatment (10 or 100 µg/ml) significantly increased the relative fraction of fibrous tissue staining blue in trichrome sections relative to vehicle treatment (B; *n*=5–7 per group).

are observed in muscle 5 days following injury in rats (Kirk et al. 2000). Moreover, our data show for the first time that myostatin is also strongly expressed in the mature and proliferating chondrocytes during endochondral ossification. We and others (Nagamine et al. 1998) have observed the myostatin receptor, Acvr2b, to be expressed in these cells as well. Taken together, these results point to an autocrine function of myostatin in soft callus chondrocytes and suggest that myostatin is a factor that is expressed in a variety of tissues besides muscle. On one hand, this result is not necessarily unexpected since other TGF-β ligands, such as GDF-5, are involved in bone healing (Axelrad et al. 2007). On the other, these findings underscore the integrated nature of musculoskeletal regeneration and point to some basic similarities in the molecules involved in both muscle and bone repair.

The decrease in endochondral bone area as well as callus bone volume with localized exogenous myostatin treatment was independent of a decrease in body mass. Although systemic myostatin treatment is known to induce cachexia in rodents (Zimmers et al. 2002) and muscle-specific overexpression of myostatin decreases muscle mass in mice (Reisz-Porszasz et al. 2003), local delivery of myostatin using a hydrogel appeared to have only local effects with no systemic changes in body weight or muscle size. The significant decrease in callus endochondral bone formation

after local exogenous myostatin treatment points to a direct role for myostatin in regulating the early fracture-healing events where chondroprogenitor cells and chondrocytes are actively differentiating or proliferating. This finding is consistent with our in vitro studies showing that myostatin treatment inhibits chondrogenesis and expression of the chondrogenic factor Sox-9 (Elkasrawy et al. 2011). It is well established that blocking myostatin signaling increases muscle mass and improves muscle regeneration, and it appears that these same inhibitors might have similar effects in bone (Bialek, 2008; Ferguson et al. 2009; Borgstein et al. 2009), underscoring the tight coupling between muscle and bone anabolism. Indeed, our earlier study utilizing a myostatin propeptide revealed that systemic injections of a myostatin inhibitor can enhance bone healing as well as muscle regeneration (Hamrick, Arounleut, et al. 2010). Evidence shows that extensive muscle tissue injury has a negative impact on early bone healing (Utvag et al. 2002), whereas open fractures show improved healing when covered with an intact muscle flap (Gopal et al. 2000). It has also been reported that fracture callus size is increased in regions where there is abundant muscle coverage (Landry et al. 2000) and that the muscle bed adjacent to the fracture site may contribute chondroprogenitor cells to the fracture hematoma (Pritchard and Ruzicka 1950). Studies of muscle regeneration (Zhu et al. 2007) as well as studies of tendon and ligament tissue (Mendias et al. 2008; Fulzele et al. 2010) suggest that myostatin is a profibrotic factor in the sense that myostatin increases the expression of TGF-β and type 1 collagen. This is consistent with our findings showing a significant dose-dependent increase in fibrotic tissue during muscle regeneration with myostatin treatment and with previous work demonstrating that myostatin treatment increases muscle fibroblast proliferation and extracellular matrix synthesis (Li et al. 2008).

The findings reported here and the previous work referenced above raise the general question of why myostatin would be expressed following injury if it appears to have such detrimental effects on bone and muscle healing. Myostatin has multiple roles during muscle development and regeneration, such as regulating myoblast proliferation and differentiation (McFarlane et al. 2011). Thus, within this context, myostatin serves as a "brake" of sorts that guides muscle growth and development to keep muscle fiber size and number within a functionally and metabolically appropriate range. In addition, myostatin stimulates the differentiation of myofibroblasts from myoblasts and enhances the deposition of fibrous collagenous tissue by these cells (Burks and Cohn 2011). In this way, myostatin also serves a short-term repair function by replacing damaged muscle tissue that is removed by macrophages with a patchwork of mechanically stable fibrous tissue. Myostatin therefore serves several important functions in normal growth, development, and repair of muscle tissue; however, in those cases where muscle damage is particularly widespread, such as extremity trauma or dystrophin deficiency, the accumulation of fibrous tissue is likely to significantly impair muscle function in the longer term. In these cases, inhibiting myostatin may be an effective therapeutic approach for enhancing muscle repair.

Blocking myostatin has been widely investigated for the treatment of muscular dystrophy (Wagner 2005; Wagner et al. 2008). Several myostatin inhibitors, such as myostatin propeptide, decoy soluble receptor, myostatin antibody, and follistatin, have been shown to enhance muscle regeneration, increase myofiber hypertrophy, and decrease fibrosis in healing muscle (Wagner 2005; Zhu et al. 2011). Our studies suggest that these inhibitors may improve not only muscle regeneration but also bone healing in cases of orthopaedic trauma. The time course data presented in this article suggest that such inhibitors may be most effective during the relatively early stages of fracture healing (e.g., inflammatory and early chondrogenic phases). Future studies should be directed at investigating potential synergies between molecules that may promote muscle repair, such as myostatin inhibitors, and molecules that may directly stimulate osteogenesis, such as BMP-2, GDF-5, and BMP-7, as well as factors that stimulate angiogenesis, such as VEGF. Fracture non-union remains a significant problem, and this problem is exacerbated in those cases where soft tissue coverage is not available or where soft tissues are significantly damaged. Integration of data on muscle healing with that on bone repair is likely to reveal new therapeutic strategies that may involve administering different therapeutics at different stages of the healing process to more effectively promote successful recovery from complex musculoskeletal injuries.

Acknowledgment

We are grateful to Dr William Hill for his assistance with fluorescence microscopy imaging; to Donna Kumiski for her assistance in the staining techniques; to Phonepasong Arounleut for his assistance in animal surgery, tissue sectioning, and ImageJ software; and to Matthew Bowser for his assistance in the lab.

Declaration of Conflicting Interests

The authors declared no potential conflicts of interest with respect to the authorship and publication of this article.

Funding

The authors disclosed receipt of the following financial support for the research and/or authorship of this article: The National Institutes of Health (AR049717), Office of Naval Research (N000140810197), and Department of the Army (USAMRMC PR093619).

References

Allen DL, Bandstra ER, Harrison BC, Thorng S, Stodieck LS, Kostenuik PJ, Morony S, Lacey DL, Hammond TG, Leinwan LL, et al. 2009. Effects of spaceflight on murine skeletal muscle gene expression. J Appl Physiol. 106:582–595.

Axelrad TW, Kakar S, Einhorn TA. 2007. New technologies for the enhancement of skeletal repair. Injury. 38 Suppl 1:S49–S62.

Bialek P, Parkington J, Warner L, St Andre M, Jian L, Gavin D, Wallace C, Zhang J, Yan G, Root A, et al. 2008. Mice treated with a myostatin/GDF-8 decoy receptor, ActRIIB-Fc, exhibit a tremendous increase in bone mass. Bone. 42:S46.

Borgstein CC, Yang Y, Wilson D, Haltom E, Lachey J, Seehra J, Sherman M. 2009. Preliminary results from single subcutaneous administration of ACE-031, a form of the soluble activin typeII B receptor, in healthy postmenopausal volunteers. Neuromuscul Disord. 19:546.

Burks T, Cohn R. 2011. Role of TGF-beta signaling in inherited and acquired myopathies. Skelet Muscle. 1:19.

Cho TJ, Gerstenfeld LC, Einhorn TA. 2002. Differential temporal expression of members of the transforming growth factor beta superfamily during murine fracture healing. J Bone Miner Res. 17:513–20.

Elkasrawy MN, Fulzele S, Bowser M, Wenger K, Hamrick MW. 2011 Jul 15. Myostatin (GDF-8) inhibits chondrogenesis and chondrocyte proliferation in vitro by suppressing Sox-9 expression. Growth Factors. 29:253–62.

Elkasrawy MN, Hamrick MW. 2010. Myostatin (GDF-8) as a key factor linking muscle mass and bone structure. J Musculoskelet Neuronal Interact. 10:56–63.

Ferguson V, Stodieck L, Hanson A, Young M, Bateman T. 2009. Inhibiting myostatin prevents microgravity-associated bone loss in mice. J Bone Miner Res. 24 Supp 1:1288.

Fulzele S, Arounleut P, Cain M, Herberg S, Hunter M, Wenger K, Hamrick MW. 2010. Role of myostatin (GDF-8) signaling in the human anterior cruciate ligament. J Orthop Res. 28:1113–1118.

Gonzalez-Cadavid NF, Taylor WE, Yarasheski K, Sinha-Hikim I, Ma K, Ezzat S, Shen R, Lalani R, Asa S, Mamita M, et al. 1998. Organization of the myostatin gene and expression in health men and HIV-infected men with muscle wasting. Proc Natl Acad Sci U S A. 95:14938–14943.

Gopal S, Majumder S, Batchelor AG, Knight SL, De Boer P, Smith RM. 2000. Fix and flap: the radical orthopaedic and plastic treatment of severe open fractures of the tibia. J Bone Joint Surg Br. 82:959–966.

Hamrick MW. 2011. A role for myokines in muscle-bone interactions. Exerc Sport Sci Rev. 39:43–47.

Hamrick MW, Arounleut P, Kellum E, Cain M, Immel D, Liang LF. 2010. Recombinant myostatin (GDF-8) propeptide enhances the repair and regeneration of both muscle and bone in a model of deep penetrant musculoskeletal injury. J Trauma. 69:579–583.

Hamrick MW, McNeil PL, Patterson SL. 2010. Role of muscle-derived growth factors in bone formation. J Musculoskelet Neuronal Interact. 10:64–70.

Hamrick MW, Shi X, Zhang W, Pennington C, Thakore H, Haque M, Kang B, Isales CM, Fulzele S, Wenger KH. 2007. Loss of myostatin (GDF8) function increases osteogenic differentiation of bone marrow-derived mesenchymal stem cells but the osteogenic effect is ablated with unloading. Bone. 40:1544–1553.

Hittel DS, Axelson M, Sarna N, Shearer J, Huffman KM, Kraus WE. 2010. Myostatin decreases with aerobic exercise and associates with insulin resistance. Med Sci Sports Exerc. 42:2023–2029.

Kellum E, Starr H, Arounleut P, Immel D, Fulzele S, Wenger K, Hamrick MW. 2009. Myostatin (GDF-8) deficiency increases fracture callus size, Sox-5 expression, and callus bone volume. Bone. 44:17–23.

Kirk S, Oldham J, Kambadur R, Sharma M, Dobbie P, Bass J. 2000. Myostatin regulation during skeletal muscle regeneration. J Cell Physiol. 184:356–363.

Landry P, Marino A, Sadasivan K, Albright J. 2000. Effect of soft-tissue trauma on the early periosteal response of bone to injury. J Trauma. 48:479–483.

Lee SJ. 2004. Regulation of muscle mass by myostatin. Annu Rev Cell Dev Biol. 20:61–86.

Li Z, Kollias H, Wagner KR. 2008. Myostatin directly regulates skeletal muscle fibrosis. J Biol Chem. 283:19371–19378.

McFarlane C, Hui G, Amanda W, Lau H, Lokireddy S, Xiaojia G, Mouly V, Butler-Browne G, Gluckman P, Sharma M, et al. 2011. Human myostatin negatively regulates human myoblast growth and differentiation. Am J Physiol Cell Physiol. 301:C195–C203.

McPherron AC, Lawler AM, Lee SJ. 1997. Regulation of skeletal muscle mass in mice by a new TGF-beta superfamily member. Nature. 387:83–90.

Mendias C, Bakhurin K, Faulkner J. 2008. Tendons of myostatin-deficient mice are small, brittle, and hypocellular. Proc Natl Acad Sci U S A. 105:388–393.

Nagamine T, Imamura T, Ishidou Y, Kato M, Murata F, ten Dijke P, Sakou T. 1998. Immunohistochemical detection of activin A, follistatin, and activin receptors during fracture healing in the rat. J Orthop Res. 16:314–321.

Ostebye TK, Bardal T, Vegusdal A, Frang OT, Kjorvsik E, Andersen O. 2007. Molecular cloning of the Atlantic salmon activin recetor IIB cDNA-localization of the receptor and myostatin in vivo and in vitro in muscle cells. Comp Biochem Physiol Part D Genomics Proteomics. 2:101–111.

Pritchard JJ, Ruzicka AJ. 1950. Comparison of fracture repair in the frog, lizard and rat. J Anat. 84:236–261.

Reisz-Porszasz S, Bhasin S, Artaza JN, Shen R, Sinha-Hikim I, Hogue A, Fielder TJ, Gonzalez-Cadavid NF. 2003. Lower skeletal muscle mass in male transgenic mice with muscle-specific overexpression of myostatin. Am J Physiol Endocrinol Metab. 285:E876–E888.

Shuto T, Sarkar G, Bronk JT, Matsui N, Bolander ME. 1997. Osteoblasts express types I and II activin receptors during early intramembranous and endochondral bone formation. J Bone Miner Res. 12:403–411.

Stein H, Perren SM, Cordey J, Kenwright J, Mosheiff R, Francis MJ. 2002. The muscle bed: a crucial factor for fracture healing: a physiological concept. Orthopedics. 25:1379–1383.

Utvag SE, Iversen KB, Grundnes O, Reikeras O. 2002. Poor muscle coverage delays fracture healing in rats. Acta Orthop Scand. 73:471–474.

Wagner KR. 2005. Muscle regeneration through myostatin inhibition. Curr Opin Rheumatol. 17:720–724.

Wagner KR, Fleckenstein JL, Amato AA, Barohn RJ, Bushby K, Escolar DM, Flanigan KM, Pestronk A, Tawil R, Wolfe GI, et al. 2008. A phase I/IItrial of MYO-029 in adult subjects with muscular dystrophy. Ann Neurol. 63:561–571.

Wehling M, Cai B, Tidball J. 2000. Modulation of myostatin expression during modified muscle use. FASEB J. 14:103–110.

Whittemore LA, Song K, Li X, Aghajanian J, Davies M, Girgenrath S, Hill JJ, Jalenak M, Kelley P, Knight A, et al. 2003. Inhibition of myostatin in adult mice increase skeletal muscle mass and strength. Biochem Biophys Res Commun. 300:965–971.

Zhu J, Li Y, Lu A, Gharaibeh B, Ma J, Kobayashi T, Quintero A, Huard J. 2011. Follistatin improves skeletal muscle healing after injury and disease through an interaction with muscle regeneration, angiogenesis, and fibrosis. Am J Pathol. 179:915–930.

Zhu J, Li Y, Shen W, Qiao C, Ambrosio F, Lavasani M, Nozaki M, Branca MF, Huard J. 2007. Relationships between transforming growth factor-betal, myostatin, and decorin: implications for skeletal muscle fibrosis. J Biol Chem. 282: 25852–25863.

Zimmers TA, Davies MV, Koniaris LG, Haynes P, Esquela AF, Tomkinson KN, McPherron AC, Wolfman NM, Lee SJ. 2002. Induction of cachexia in mice by systemically administered myostatin. Science. 296:1486–1488.